ELSEVIER

International Journal of Pharmaceutics 228 (2001) 19–31

international journal of pharmaceutics

www.elsevier.com/locate/ijpharm

Production of griseofulvin nanoparticles using supercritical CO_2 antisolvent with enhanced mass transfer

Pratibhash Chattopadhyay, Ram B. Gupta *

Department of Chemical Engineering, Auburn University, Auburn, AL 36839-5127, USA

Received 19 February 2001; received in revised form 3 July 2001; accepted 5 July 2001

Abstract

Griseofulvin (GF) is a poor water soluble, antifungal agent. The bioavailability of the drug and its absorption from the gastrointestinal tract can be greatly improved by particle size reduction. In this work, supercritical antisolvent precipitation with enhanced mass transfer (SAS-EM) has been proposed for the production of GF nanoparticles. SAS-EM is a modification of the currently existing supercritical antisolvent (SAS) precipitation technique and also utilizes supercritical CO_2 as the antisolvent. In SAS-EM however, the solution jet is deflected by a surface vibrating at an ultrasonic frequency that atomizes the jet into small micro droplets. Further, the ultrasound field generated by the vibrating surface inside the supercritical media enhances mass transfer and prevents agglomeration due to increased mixing. GF nanoparticles of different sizes and morphologies have been obtained by varying the vibration intensity of the deflecting surface, which in turn is adjusted by changing the power supply to the attached ultrasound transducer. GF nanoparticles as low as 130 nm in size have been obtained corresponding to a power supply of 180 W. The effect of using different solvents on the size and morphology of the particles has also been studied. © 2001 Elsevier Science B.V. All rights reserved.

Keywords: Griseofulvin; Supercritical CO_2; Antisolvent; Ultrasound; Nanoparticles

1. Introduction

Griseofulvin (GF) is an orally administered, antibiotic and antifungal drug. Although this drug is widely used for the treatment of mycotic diseases of the skin, hair and nails, it has problems with safety and efficiency since its therapeutic dose is fairly close to its toxicity limit. GF has a very low solubility in water (15 μg/ml at 37 °C) and hence it has low bioavailability and exhibits variable and incomplete absorption through the gastrointestinal tract (GIT). Since for any drug, certain minimal drug–plasma levels are needed for it to be effective, GF preparations have to be carefully designed for maximum absorption. Another limitation due to the low solubility and poor bioavailability of GF is difficulty in the determination of an effective dosage of the drug required for proper treatment. (Mathews and Rhodes, 1967). For example, Sharpe and Tomich (1960) were unable to determine a lethal dose of orally

* Corresponding author. Tel.: +1-334-844-2013; fax: +1-334-844-2063.

E-mail address: gupta@auburn.edu (R.B. Gupta).

0378-5173/01/$ - see front matter © 2001 Elsevier Science B.V. All rights reserved.
PII: S0378-5173(01)00803-1

administered GF in rats and mice and Gonzalez-Ochoa and Ahumada-Padilla (1959) had similar problems with the treatment of dermatophytoses in man.

An effective method of increasing the solubility of any drug, whether readily or sparingly soluble in water, is through comminution of the drug into fine particles. Small micron size particles have higher dissolution rates due to increased surface area. Apart from that, particles smaller than 1 μm also have higher saturation solubilities and a better adhesion to the walls of the GIT, which enhances bioavailability (Diederich and Muller, 1998). Several attempts have been made in order to investigate the effect of particle size on the absorption of GF in humans and animals after oral administration. Atkinson et al. (1962) observed that with increase in the specific area of GF particles from approximately 0.4 (mean particle diameter of 10 μm) to 1.5 (mean particle diameter 2.7 μm), the effective absorption of GF is almost doubled. Kraml et al. (1962) found that a 0.5-g dose of micronized GF produced serum levels indistinguishable from those by a 1.0 g dose of non-micronized GF.

A number of techniques have been developed in past for the manufacture of micronized drug particles, including spray drying (Nass, 1988) and ultra fine milling (Hixon et al., 1990; Van Cleef, 1991). The major disadvantage of these techniques is that a broad size distribution of particles (0.5–25 μm) is obtained and only a small fraction of the particles are produced in the micron or nanometer range (Reverchon et al., 1998). Drug nanoparticles can also be prepared using the precipitation process employing liquids as antisolvent, which leads to the formation of hydrosols. The primary limitations of the liquid antisolvent technique include difficulties in containing and controlling particle growth, and effective elimination of the liquid solvents from the drug particles.

In recent years, supercritical fluid technologies such as Rapid Expansion of Supercritical Solutions (RESS) and Supercritical Antisolvent (SAS) precipitation have emerged as attractive methods for drug particle formation. Advantages of these techniques include mild operating temperatures and the production of solvent free particles. The particles obtained by these techniques are 0.7–5.0 μm in size and have a narrow size distribution. Several researchers have attempted the precipitation of GF particles using these supercritical fluid technologies. The results obtained so far have not been promising since in most of the cases, several microns long, needle shaped crystals of GF have been obtained. (Chen et al., 2001; Reverchon et al., 1995; Reverchon and Della Porta, 1999). For example, Reverchon et al. (1995) precipitated quasispherical crystals of GF particles around 1.1 μm in size using the RESS technique with CHF_3 as the solvent, but later using the SAS technique they again observed long needle shaped crystals some millimeters in length for different solvents such as dichloromethane and dimethylsulfoxide (Reverchon, 1999).

We have proposed a new technique (Gupta and Chattopadhyay, 2000; Chattopadhyay et al., 2001) that can be used to manufacture GF particles in the nanometer and micrometer ranges having a fairly narrow size distribution. The new technique, supercritical antisolvent with enhanced mass transfer (SAS-EM), is a modification of the conventional SAS process and overcomes the currently existing limitations of the SAS process. The main modification in the new technique is that it utilizes a deflecting surface, vibrating at an ultrasonic frequency to atomize the solution jet into micro-droplets, or to further break the particle jet into smaller particles. The ultrasound field generated by the horn surface also provides a velocity component in the y-direction (direction normal to the horn surface) that greatly enhances turbulence and mixing within the supercritical phase, resulting in a high mass transfer between the solution and the antisolvent. The combined effect of fast rate of mixing between the antisolvent and the solution, and the reduction of solution droplet size due to atomization, provides particles approximately 10-fold smaller than those obtained from the conventional SAS process. Table 1 illustrates the broad differences between the SAS and the SAS-EM techniques for particle production.

In this work, we examine the use of the SAS-EM technique for the precipitation of GF nanoparticles. The precipitation process is carried out using two different solvents. The process

parameter, power supply to the ultrasound transducer and its effect on particles size, is investigated. The morphology of particles obtained from each of the experiments is also characterized.

2. Experiment

2.1. Materials

CO_2 and N_2 (both 99.9% pure) from Airco, griseofulvin (95% pure, lot no. 115H1180) from Sigma, tetrahydrofuran (THF, 99.9% pure) from Fisher Scientific, and dichloromethane (DCM, 99.9% pure) from Fisher Scientific were used as received.

2.2. Apparatus

A schematic representation of the SAS-EM apparatus is shown in Fig. 1. The main component of the apparatus consists of a high-pressure ultrasound precipitation cell (R) approximately 80 cm^3 in volume. A titanium horn (H) (Sonics and Materials, Inc) having a tip 1.25 cm in diameter is attached to the precipitation cell to provide the ultrasonic field, which in turn is generated by a 600 W (max. power), 20 kHz ultrasonic processor (U, Ace Glass, Inc). The ultrasonic processor is designed to deliver constant amplitude. A collection plate is placed inside the precipitation cell for collecting the particles. High pressure inside the cell is generated using an ISCO syringe pump. Temperature inside the precipitation cell is maintained by placing it in a constant temperature water bath. The solution containing the solid to be precipitated is injected inside the precipitation cell using a 'solution injection device' (S), which consists of a stainless steel cylinder containing a piston. The piston divides the cylinder into two chambers. The GF solution is placed inside one of these chambers and is delivered into the cell by using pressurized nitrogen in the other chamber. The device S is connected to the vessel by means

Table 1
Differences between the conventional SAS technique and the new SAS-EM technique

SAS technique	SAS-EM technique
Droplet formation	
Droplet formation is due to jet break up of the solution jet that is injected into the supercritical fluid phase medium	Droplet formation is due to atomization of the jet into micro-droplets by the vibrating horn surface at an ultrasonic frequency of 20 kHz
Mass transfer rate	
Depends on the solvent in use and is the rate of transfer of the solvent between the droplet and the super critical fluid medium	Also depends on the solvent in use, but there is an enhanced rate of mass transfer between the droplet and the supercritical fluid due to increased mixing and turbulence caused by the ultrasonic field
Droplet/particle motion	
Droplet/particle motion within the supercritical fluid phase is due to the momentum imparted by the solution jet velocity	Droplet/particle motion within the supercritical fluid phase is due to the vibrating ultrasonic surface, which propels the droplets away from the horn at a rapid rate
Particle sizes obtained	
Sizes of the particles obtained are fairly small, in the micrometer range (1–5 μm)	Sizes of the particles obtained by this method are smaller, in the nanometer range (100–500 nm)
Particle size adjustability	
Particles sizes and morphology can be slightly controlled by changing the density of the supercritical fluid by varying the pressure and the temperature of the supercritical fluid	Particle sizes and morphology can be controlled to a great extent by changing the power supplied to the vibrating surface (i.e. changing the amplitude of the vibrating surface). In addition, a minor control can also be obtained by changing supercritical fluid density

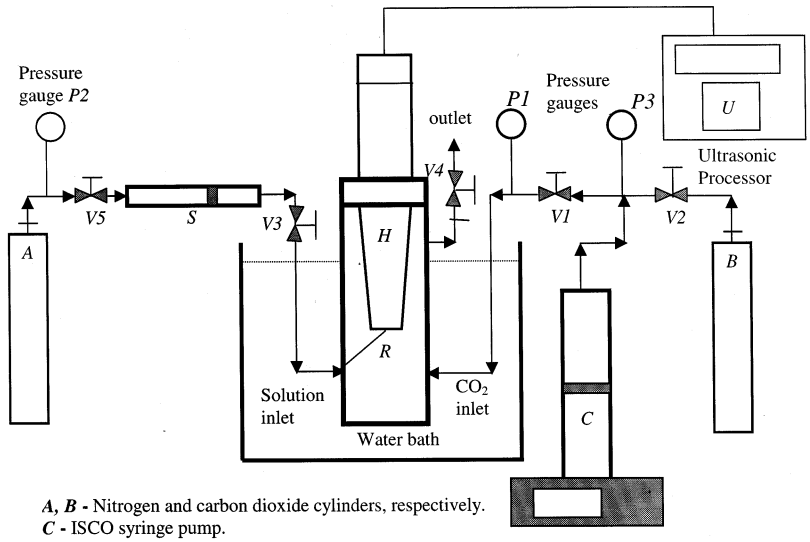

A, B - Nitrogen and carbon dioxide cylinders, respectively.
C - ISCO syringe pump.
V, P - Control valves and Pressure gauges.
S - Solution injection system, a piston device.
R - High-pressure precipitation cell.
H - Titanium Horn
U - Ultrasonic Processor

Fig. 1. Schematic representation of the SAS-EM apparatus for Griseofulvin particle precipitation.

of a 75-μm i.d. fused silica capillary tube. A pressure drop of 41 bars is maintained across the capillary tube and the device S in order to spray the solution inside the precipitation cell. The capillary tube is placed at an angle of 40° with respect to the horn surface in a manner such that the capillary opening just touches the horn surface. Supercritical CO_2 is fed inside the precipitation cell through the inlet port located at the bottom of the vessel. Valve V1 is used to control the flow of Supercritical CO_2 into the high-pressure cell. Pressure inside the cell is measured using a pressure gauge P1. The outlet port is located on top of the precipitation cell and valve V4 is used to control the depressurization process. The pressure difference across the capillary and the device S is measured using the pressure gauges P2 and P1.

2.3. Procedure

All the precipitation experiments were carried out in the batch mode and in an identical manner at 96.5 bar and at 35 °C. The vibration frequency of the horn surface was kept constant at 20 kHz and the amplitude of vibration of the horn surface was varied by changing the power supply to the ultrasound transducer. Precipitation was achieved using two different solvents, DCM and THF.

First, the ultrasonic precipitation cell was filled with carbon dioxide up to desired operating pressure. The temperature inside the cell was maintained constant using a water bath. Approximately, 2.5 g of the GF solution (5 mg/ml) was then loaded into the 'solution injection device' (*S*) ready to be injected into the precipitation cell. The ultrasonic horn inside the cell was then switched on at the desired amplitude by adjusting the input power, and the solution was introduced inside the precipitation cell through the 75 μm fused silica capillary tube, placed against the horn surface at an angle of 40°. As soon as the solution jet was in contact with the horn surface, it was atomized into tiny droplets and particles were formed due to the rapid removal of the solvent by supercritical CO_2 from these droplets. The particles were in constant motion due to the ultrasonic field generated by the horn surface inside the precipitation cell, thereby

preventing agglomeration. The injection process was typically completed in 2–3 min and the power supply to the ultrasonic horn was turned off thereafter.

Next was the washing step in which the residual solvent, left dissolved in supercritical CO_2, was removed by continuously purging the precipitation cell with fresh CO_2. The complete cleaning process required approximately seven to eight times the vessel volume of fresh CO_2. The precipitation cell was then allowed to slowly depressurize to ambient pressure. The cell was then opened and the collection plate was removed and taken for particle analysis.

2.4. Analysis

2.4.1. Particle size distribution

Size analysis was carried out using scanning electron microscopy (SEM, Zeiss, model DSM940). For analysis, portions of the collection plate were cut and were coated with gold/palladium using a sputter coater (Pelco, model Sc-7). SEM micrographs of different regions of the collection plate were obtained in order to get the nearest possible representation of the size distribution of all the particles. From the SEM micrographs, the volume particle size distribution, the number average and standard deviation (S.D.) of the particles were determined by measuring the diameters of about 100–200 randomly selected particles for each experiment. The purpose of size determination using the SEM micrographs was not to come up with an accurate measurement of the particle size but to prove that the SAS-EM technique can indeed be used for GF nanoparticle production.

3. Results

The observed morphologies of particles obtained from each of the experiments are summarized in Table 2. Fig. 2a–f and Fig. 4a–e are SEM micrographs of particles obtained from experiments conducted at the different horn amplitudes using DCM and THF as solvents, respectively.

When DCM was used as the solvent and when there was no power supply to the transducer, long needle shaped crystals of GF several millimeters in length were obtained (Fig. 2a). It is important to note here that experiments conducted with no ultrasound were basically the SAS process. Results obtained in this case were similar to the ones obtained by Reverchon and Della Porta (1999) during their SAS experiments. As the power supply to the ultrasound transducer was increased, a mixture of long needle shaped crystals of GF and small nearly spherical shaped, elongated GF nanoparticles (referred to as GF nanoparticles here after) were obtained. Fig. 3a–d are SEM micrographs of the GF nanoparticles obtained from each of these experiments corresponding to different values of total power supply to the transducer. When the total power supply was 90 W, narrower and shorter needle shaped crystals of GF were obtained (Fig. 2c). A low yield of GF nanoparticles (Fig. 3a) was also obtained, but most of the solid was in the form of long needle shaped crystals 50 μm long and 2.5 μm wide.

As the power supply to the transducer was increased, a drastic change in the morphology of the particles was observed. A relatively small amount of long needle shaped GF crystals were obtained when the total power supply to the transducer was 120 W. The volumetric mean of the GF nanoparticles obtained in this case was 130 nm (Fig. 3b) while the larger needle like GF crystals were 7.3 μm long and 2.7 μm wide (Fig. 2d). With increase in the power supply beyond 120 W there was a further increase in the yield of GF nanoparticles formed. The volumetric mean of the GF nanoparticles obtained corresponding to 150 W total power supply was 520 nm (Fig. 3c) while the larger needle like GF crystals were 3.8 μm long and 1.4 μm wide (Fig. 2e). At 180 W power supply the volumetric mean of the obtained GF nanoparticles was 310 nm (Fig. 3d). Large GF needle shaped crystals 2.0 μm long and 1.6 μm wide were also obtained having a low yield (Fig. 2f).

When THF was used as the solvent, with no power supply to the transducer, several millimeters long fibers of GF were obtained (Fig. 4a). When the total power supply was increased to 90

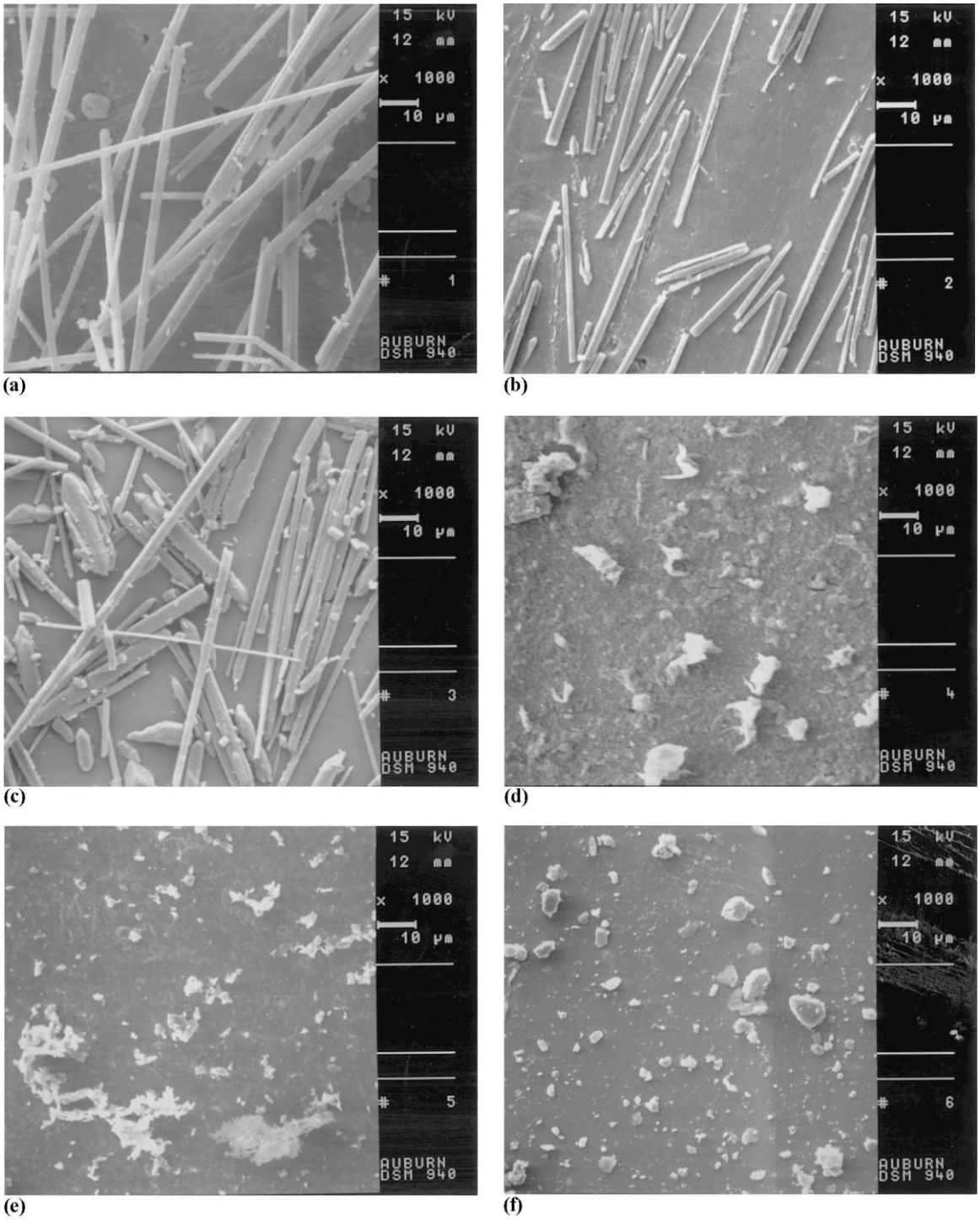

Fig. 2. SEM micrographs showing the change in the morphologies of GF particles obtained from experiments conducted at different values of power supply using DCM as solvent. (a) No power supply, (b) 60 W power supply, (c) 90 W power supply, (d) 120 W power supply, (e) 150 W power supply, (f) 180 W power supply. Magnification is $\times 1000$

W, there was a change in the morphology of the particles and long needle shaped crystals of GF 45 μm long and 2.5 μm wide were obtained (Fig. 4b). As the power supply was further increased to 120 W, there was again a change in the morphology of the particles and a mixture of GF nanoparticles and long needle shaped crystals of GF were obtained. Fig. 5a–c are SEM micrographs of the GF nanoparticles obtained from each of these experiments corresponding to different values of power supply. The volumetric mean size of GF nanoparticles was 200 nm (Fig. 5a) while the mean size of the needle shaped GF crystals was 8.0 μm long and 1.0 μm wide (Fig. 4c). The volumetric mean of the GF nanoparticles when the power supply was 150 W was 280 nm (Fig. 5b) while the mean size of the needle shaped GF crystals was 3.8 μm long and 1.6 μm wide (Fig. 4d). At 180 W power supply, GF nanoparticles having a volumetric mean size of 210 nm (Fig. 5c) were obtained. Very few larger needle shaped GF particles 2.1 μm long and 1.7 μm wide were also obtained (Fig. 4e).

3.1. Effect of the vibration intensity of the deflecting surface on the size and morphology of GF particles

From the above results it is interesting to note that, with an increase in the power supply (i.e. an increased horn vibration amplitude), there is an increase in the yield of GF nanoparticles formed. Also, there is a decrease in both the size and the yield of the larger needle shaped GF crystals, as illustrated in Fig. 2a–f, Fig. 4a–e Fig. 6a and b.

Table 2
Results of the experiments conducted at different ultrasound power at 96.5 bar and 35 °C

Solvent	Power supply (W)	Morphology of GF particles obtained	Volume-avg. size (Sph. GF particles) (nm)	Mean size of needle shaped GF crystals
DCM	0	Long needle shaped GF crystals	–	Several mm long
DCM	60	Shorter needle shaped GF crystals. Very low yield of GF nanoparticles also obtained	–	1.5 mm long, 0.01 mm wide
DCM	90	Even shorter needle shaped GF crystals. Low yield of GF nanoparticles obtained	510	50 μm long, 2.5 μm wide
DCM	120	Predominantly GF nanoparticles formed. Few short needles shaped GF nanoparticles	130	7.3 μm long, 2.7 μm wide
DCM	150	Larger yield of GF nanoparticles. Very few Shorter needle shaped GF nanoparticles also formed	520	3.8 μm long, 1.4 μm wide
DCM	180	Predominantly GF nanoparticles formed. Low yield of short needle shaped GF particles	310	2.0 μm long, 1.6 μm wide
THF	0	Long fibers of GF several millimeters long	–	–
THF	90	Long needle shaped GF crystals	–	45.0 μm long, 2.5 μm wide
THF	120	Shorter needle shaped GF crystals. Low yield of GF nanoparticles also obtained	200	8.0 μm long, 1.0 μm wide
THF	150	Predominantly GF nanoparticles formed. Low yield of short needle shaped GF crystals formed	280	3.8 μm long, 4.6 μm wide
THF	180	Larger yield of GF nanoparticles. Low yield of shorter needle shaped GF crystals also formed	210	2.1 μm long, 1.7 μm wide

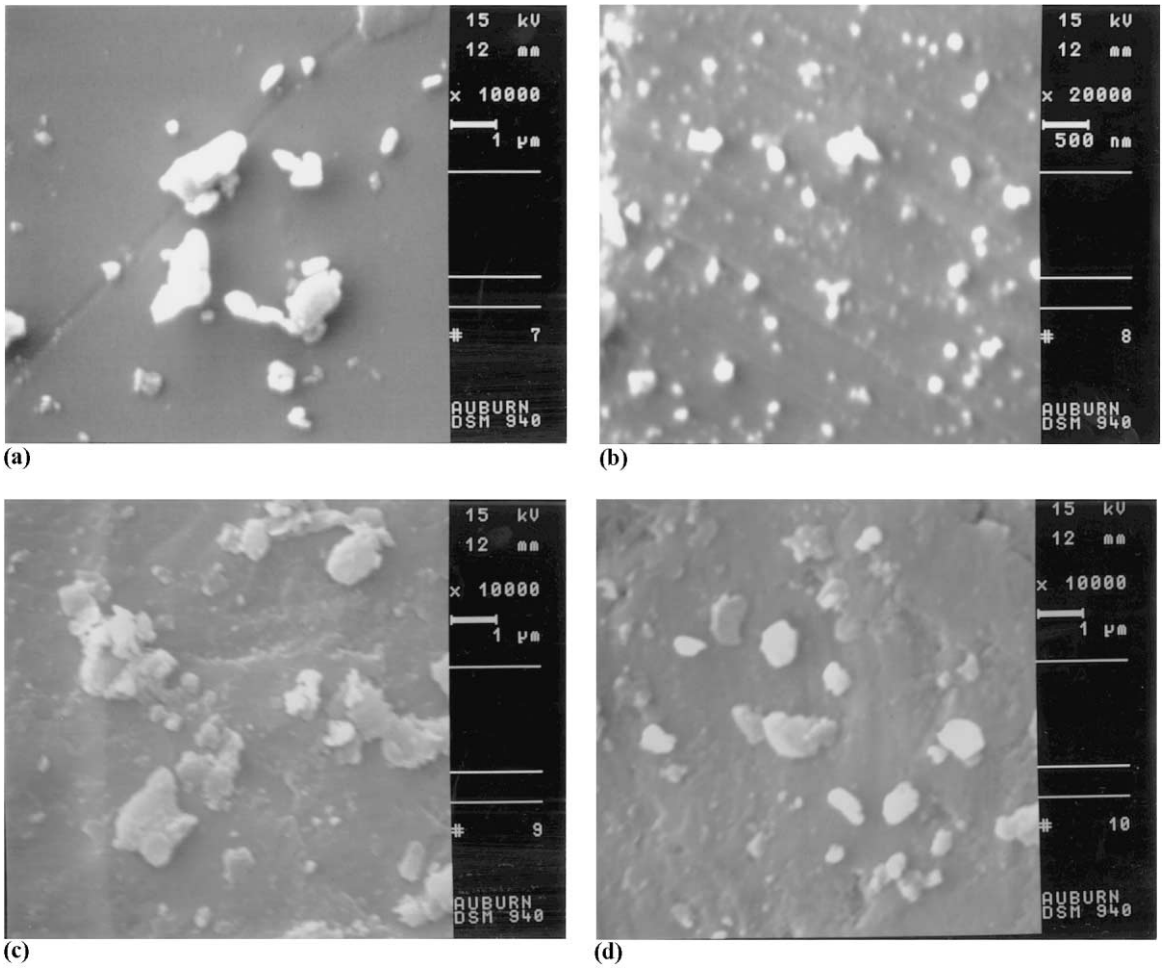

Fig. 3. SEM micrographs of spherical shaped GF nanoparticles obtained from experiments conducted at different values of power supply using DCM as solvent. (a) 90 W power supply, × 10,000, (b) 120 W power supply, × 20,000, (c) 20,000 150 W power supply, × 10,000. (d) 180 W power supply, × 10,000.

Here upon visual inspection one can see a change in the morphology of the particles and also a decrease in the yield of large needle shaped GF crystals with increased power supply. Fig. 7 shows the relationship between the mean size of GF nanoparticles and power supply to the transducer. GF nanoparticles having a volumetric mean as low as 130 nm have been obtained corresponding to 120 W power supply when DCM was used as the solvent. Increase in GF nanoparticle size thereafter was due to an increase in the proportion of GF nanoparticles obtained. Fig. 8 shows the relationship between the volume of the large needle shaped GF crystals and ultrasound power supply. There is a considerable decrease in the volume of the long needle shaped GF crystals with increasing power supply in case of both the solvents. Although based on Figs. 7 and 8, no particular trend can be established about the effect of the solvent on the size and morphology of GF particles, they do help in illustrating how ultrasound power supply causes a reduction in the yield of larger needle shaped crystals and an increase in the yield of the GF nanoparticles. Note that in all cases, the volume of the GF nanoparticles was computed assuming them to be spheres and the volume of the long needle shaped crystals was computed assuming them to be long cylinders.

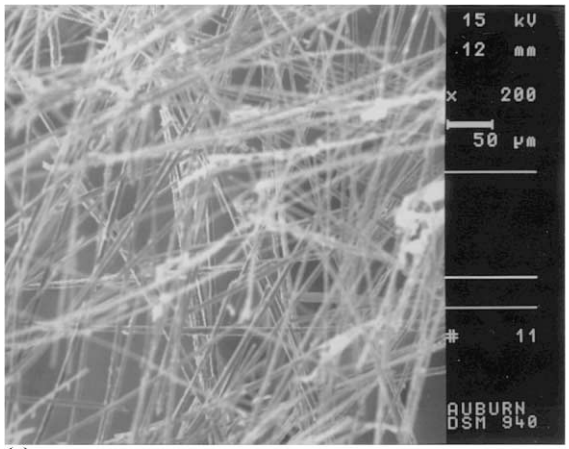

(a)

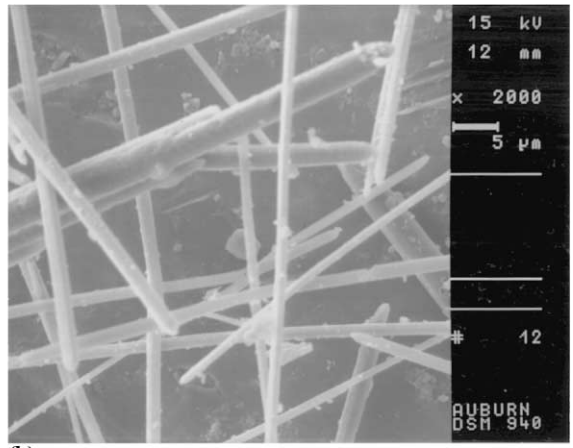

(b)

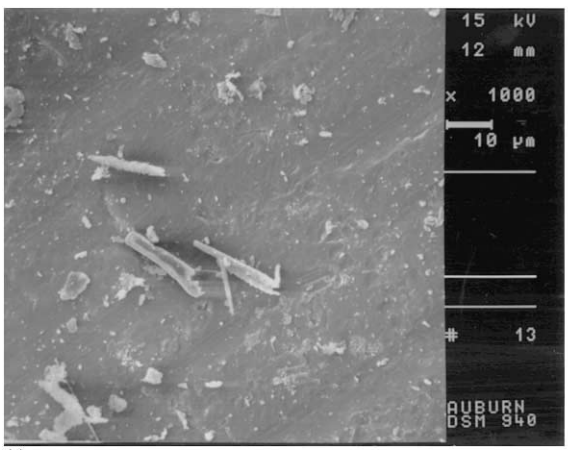

(c)

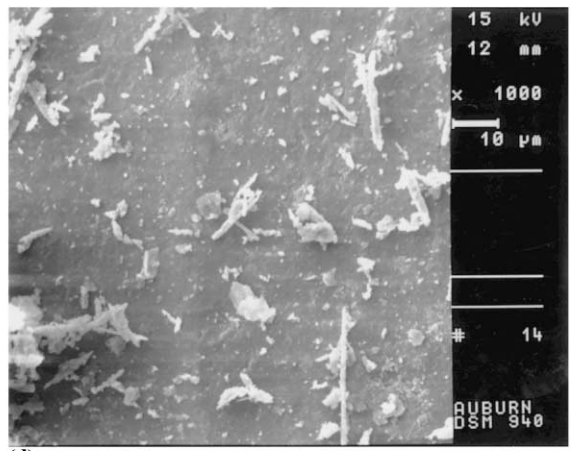

(d)

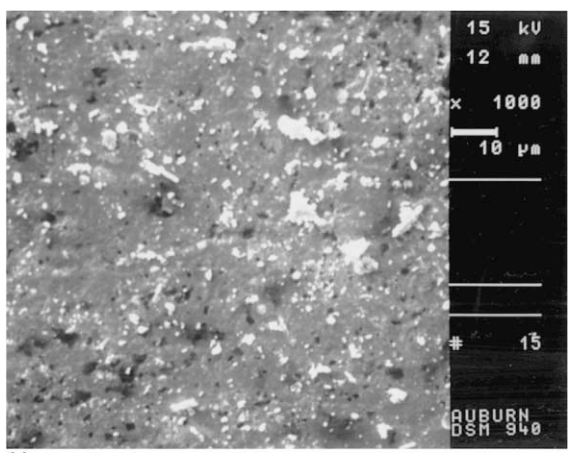

(e)

Fig. 4. SEM micrographs showing the change in the morphologies of GF particles obtained from experiments conducted at different values of power supply using THF as solvent. (a) No power supply, × 100 (b) 90 W power supply, × 2000, (c) 120 W power supply, × 1000. (d) 150 W power supply, × 1000, (e) 180W power supply, × 1000.

4. Discussion

Major factors responsible for size reduction in the SAS-EM technique are the droplet size reduction due to ultrasonic atomization and the increased mixing due to ultrasonic streaming. As soon as the GF solution is injected into the precipitation cell and onto the horn surface, the liquid spreads evenly over the surface forming a thin liquid film. Due to vibrations of the horn surface, a grid of intersecting capillary wavelets arise on the surface of this liquid film (Bindal et al., 1986). Continued oscillatory vibrations cause the height of these wavelets to increase until the tips break off and escape out as small droplets. The wavelength of these surface waves is given as

$$\lambda^3 = 2\pi\frac{\sigma}{\rho f^2} \quad (1)$$

where, f is the frequency in Hz and σ and ρ are the surface tension and the density of the fluid, respectively. The droplet diameter is proportional to the wavelength on the liquid film surface and can be determined as (Topp, 1973)

$$D = 0.34\left(\frac{8\pi\sigma}{\rho F^2}\right)^{1/3} \quad (2)$$

where, σ is the surface tension, ρ is the density of the liquid and F is the vibration frequency. Once the droplets have been formed inside the supercritical fluid, rapid transfer of CO_2 into these droplets and the solvent out of these droplets causes the droplets to expand rapidly. This subse-

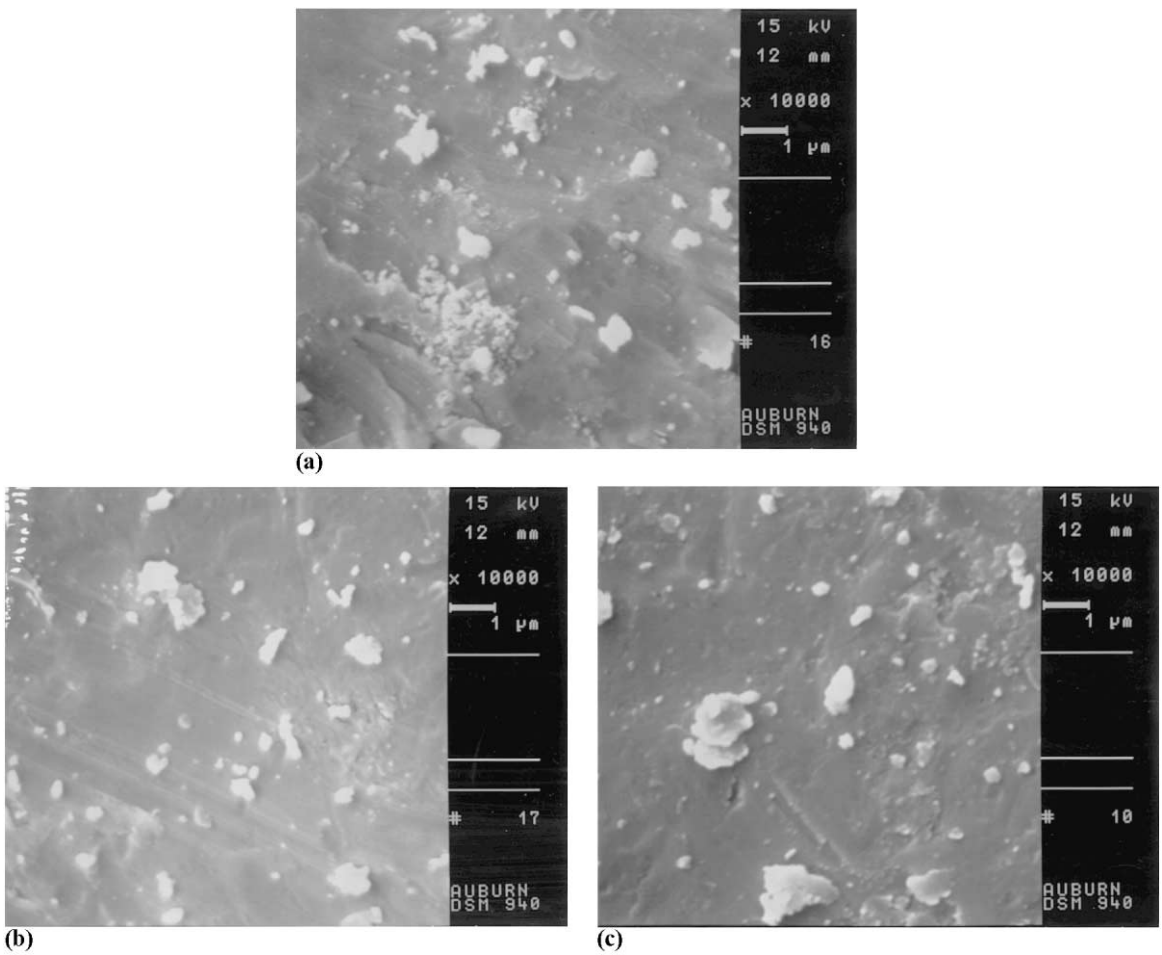

Fig. 5. SEM micrographs of spherical shaped GF nanoparticles obtained from experiments conducted at different values of power supply, using THF as solvent. (a) 120 W power supply, (b) 150 W power supply, (c) 180 W power supply. Magnification is × 10,000.

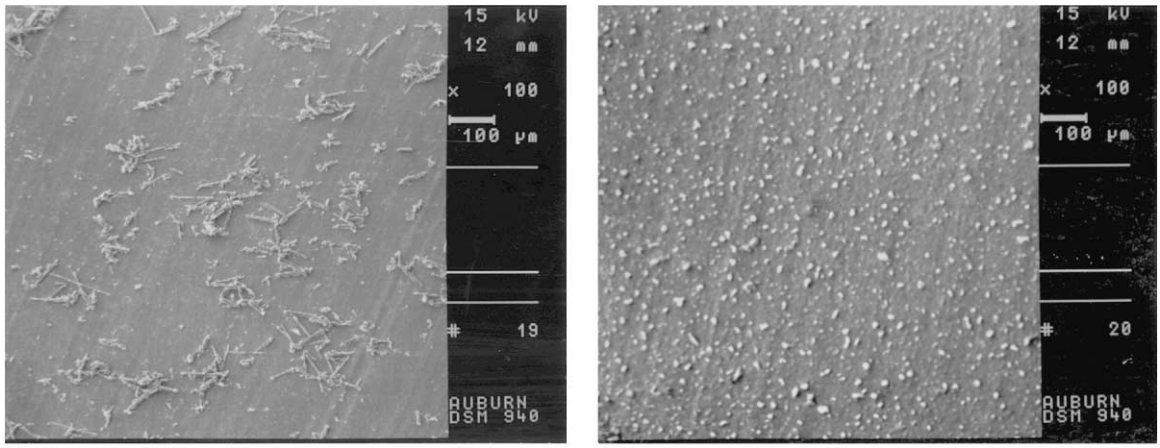

Fig. 6. SEM micrographs illustrating the change in the morphology of the particles with increasing power supply to the transducer using DCM as solvent. (a) 60 W power supply, (b) 120 W power supply. Magnification is $\times 100$.

quently decreases the droplet's ability to keep GF dissolved within it, causing GF to precipitate out as fine particles or crystals.

Another important factor that determines particle size is the mass transfer rate of the supercritical fluid into the liquid droplet. Rapid mass transfer between supercritical CO_2 and the solvent causes particles to precipitate out as tiny nuclei, which in turn coalesce together forming larger particles. Thus, better mixing characteristics can affect particle size by enhancing mass transfer rates between the solution and the supercritical phase and also by preventing the particles from agglomerating together (Palakodaty and York, 1999).

Several researchers (Mandralis and Feke, 1993; Apfel, 1990; Schram, 1988) have demonstrated that ultrasonic standing waves at appropriate intensities can increase particle motion due to the non-uniform distribution of pressure and velocity components in the standing ultrasonic wave field. This phenomenon is also observed in the SAS-EM technique. The ultrasound field provides a velocity component in the y-direction, which greatly enhances turbulence within the supercritical phase resulting in a high mass transfer due to increasing mixing. Increased mixing also helps in preventing particle agglomeration.

Propagation of the ultrasonic waves within the supercritical fluid is accompanied by a phenomenon known as acoustic or ultrasonic streaming. This phenomenon develops in a free non-uniform acoustic field or near various obstacles due to energy loss in the sound waves. The viscous forces due to the fluid medium, tend to stabilize this streaming (Shutilov, 1988). In the SAS-EM technique when the horn surface is made to vibrate at fixed amplitude, flow of liquid is away from the vibrating surface and is accompanied by inflow from regions where the liquid encounters a solid obstacle. As a result, continuous stationary circulating currents or streams are generated which keep the particles in constant motion. The three main types of acoustic streaming that are possible are large scale streaming arising in a free non-homogenous acoustic field,

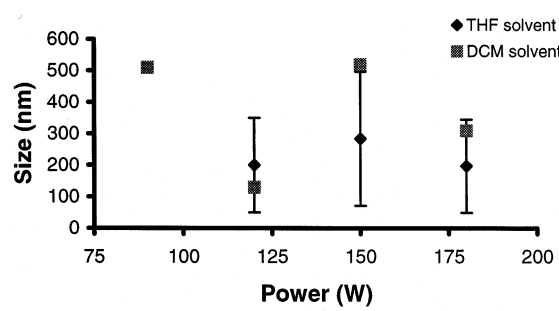

Fig. 7. Volumetric-mean size of the precipitated GF nanoparticles versus total power supply to the ultrasound transducer, for power > 75 W.

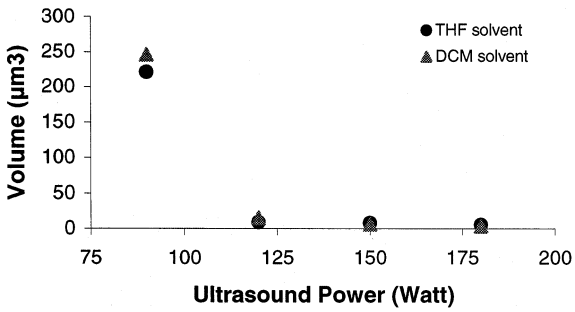

Fig. 8. Volume of long needle shaped GF crystals obtained versus power supply to the ultrasound transducer, for power >75 W.

streaming in a medium confined by rigid walls and low scale vortices arising in a viscous boundary layer near obstacles (Amramov, 1998). Depending on the ultrasonic intensity and the size of the vessel these streams are laminar or turbulent. At high ultrasonic intensities, the acoustic flow becomes extremely turbulent and gives rise to intense mixing within the supercritical fluid, which greatly enhances the rate of mass transfer between the solvent and the supercritical medium leading to precipitation of small particles.

Legsfeld et al. (2000) propose that the mechanism of particle formation in SAS process is due to particle growth in the gaseous plume, and not due to the jet atomization into droplets. Since the surface tension decreases to a negligible value within about 1 μm distance, which is smaller that the characteristic breakup lengths, the jet spreads in a fashion characteristic of a gaseous jet and microparticle formation results due to gas phase nucleation and growth within the expanding plume, rather than nucleation within discrete liquid droplets. If above theory is correct than the SAS-EM technique is working by providing a high degree of mixing causing a reduction in the particle growth.

4.1. Ultrasonic forces on the precipitated GF particles

Apart from the motion of GF particles inside the precipitation cell due to ultrasonic streaming, other forces such as gravitational, mechanical, acoustic-radiation-pressure, and hydrodynamic forces also act on the particles due to the ultrasonic field. Suspended GF particles experience mechanical forces when they encounter the vibrating surface of the horn. These forces may break the larger needle shaped crystals into smaller sizes or may also propel them away from the horn surface causing them to move around in the supercritical phase. It should be noted here that the mechanical grinding effect causing size reduction is usually more efficient for harder and large size particles and much less so for soft and smaller particles.

Acoustic radiation pressures is the difference between the average pressure at a surface moving with the displacement due to the sound and the pressure that would have existed in a fluid of the same mean density at rest (Rayleigh and Strutt, 1896). The acoustic radiation pressure force drives the GF particles to nodes (or anti-nodes) of a stationary-sound field generated inside the precipitation cell.

GF particles, suspended in the ultrasonic field oscillate with different velocities and phases relative to one another and as a result they experience a hydrodynamic force known as Bjerknes force (Lamb, 1945). Bjerknes forces acting between the particles can be attractive or repulsive depending on the value of the phase difference between the particle velocities. Another type of hydrodynamic force that the GF particles can experience is the Bernoulli's force, which is responsible for the coagulation of particles at high-frequency ultrasonic fields (Mednikov, 1963).

5. Conclusions

SAS-EM technique can be successfully used to precipitate GF nanoparticles as low as 130 nm in size. A conventional SAS process yields long needle shaped GF crystals several millimeters in length. Using the SAS-EM technique one can obtain a mixture of nearly spherical nanoparticles and micron size needle shaped crystals of GF. Effect of ultrasound power supply to the transducer on the size and the morphology of the particles have been examined. An increase in the yield of nearly GF nanoparticles and a decrease in

the yield of long needle shaped GF crystals with increase in power supply was observed. The volume of the needle shaped GF crystals decreases with increasing power supply. Hence, narrower and shorter needle shaped crystals were obtained at higher power supply to the ultrasound transducer.

Acknowledgements

Financial support from NSF (CTS-9801067) and NIH (James A. Shannon Director's award to Ram B. Gupta, 1R55RR13398-01) is appreciated. Authors are also thankful to Dr Lalit Chordia of Thar Designs, Inc (www.thardesigns.com) for technical discussions.

References

Amramov, O.V., 1998. High-Intensity Ultrasonics: Theory and Industrial Applications. Gordon and Breach Science Publishers, Amsterdam.

Apfel, R.E., 1990. Radiation Pressure-Principles and Application to Separation Science. Fortschritte der Acustik DAGA, 19, Wien.

Atkinson, R.M., Bedford, C., Child, K.J., Tomich, E.G., 1962. Effect of particle size on blood—griseofulvin levels in man, Nature February 10.

Bindal, V.N., Jain, S.K., Kumar, Y., 1986. Performance characteristics of an ultrasonic atomizer. Indian J. Technol. 24, 153–156.

Chattopadhyay, P., Gupta, R.B., 2001. Production of antibiotic nanoparticles using supercritical CO_2 as antisolvent with enhanced mass transfer. Ind. Eng. Chem. Res. 40(16), 3530–3539.

Chen, H., Lai, J., Deng X., Dai G., 2001. Fine Griseofulvin particles formation by rapid expansion of supercritical solutions. Huagong Xuebao (Chin. Ed.) 52 (1), 56–60.

Diederich, J.E., Muller, R.H., 1998. Future Strategies for Drug Delivery with Particulate Systems. Med Pharm Scientific Publishers, Berlin.

Gonzalez-Ochoa, A., Ahumada-Padilla, M., 1959. AMA Arch. Dermatol. 81, 833.

Gupta, R.B., Chattopadhyay, P., 2000. Method of forming Nanoparticles and Microparticles of Controllable size using Supercritical Fluids and Ultrasound. US Provisional Patent 60/206,644.

Hixon, L., Prior, M., Prem, H., Van Cleef, J., 1990. Sizing materials by crushing and grinding. Chem. Eng. 97, 99.

Kraml, M., Dubuc, J., Guadry, R., 1962. Proc. R. Soc. London 12, 239.

Lamb, H., 1945. Hydrodynamics. Dover Publications, New York.

Legsfeld, C.S., Delplanque, J.P., Barocas, V.H., Randolph, T.W., 2000. Mechanism governing microparticle morphology during precipitation by a compressed antisolvent: atomization vs. nucleation and growth. J. Phys. Chem. B 104, 2725–2735.

Mandralis, Z.I., Feke, D.L., 1993. Fractionation of suspensions using synchronized ultrasonic and flow fields. AIChE J. 39, 197–205.

Mathews, B.A., Rhodes, C.T., 1967. Particle size of commercial griseofulvin with reference to official standards. J. Pharma. Sci. 7, 56.

Mednikov, E.P., 1963. Acoustic coagulation and settling of aerosols. Moscow.

Nass, R., 1988. Pharmaceutical suspensions. In: Lieberman, H.A., Rieger, M., Banker, G. (Eds.), Pharmaceutical Dosage Forms. Marcel Dekker, New York, p. 151.

Palakodaty, S., York, P., 1999. Phase behavioral effects on particle formation process using supercritical fluids. Pharma. Res. 16, 976–985.

Rayleigh, B, Strutt, J.W., 1896. Theory of Sound. Macmillan and Co, New York.

Reverchon, E., 1999. Supercritical antisolvent precipitation of micro- and nano- particles. J. Supercritical Fluids 15, 1–21.

Reverchon, E, Della Porta, G., 1999. Production of antibiotic micro- and nanoparticles by supercritical antisolvent precipitation. Powder Technol. 106, 23–29.

Reverchon, E., Della Porta, G., Taddeo, R., Pallado, P., Stassi, A., 1995. Solubility and micronization of griseofulvin in supercritical CHF_3. Ind. Eng. Chem. Res. 34, 11.

Reverchon, E., Della Porta, G., Trolio, A.D., Pace, S., 1998. Supercritical antisolvent precipitation of nanoparticles of superconductor precursors. Ind. Eng. Chem. Res. 37, 952–958.

Schram, C.J., 1988. Manipulation of Particles, US Patent No. 4,743,351.

Sharpe, H.M., Tomich, E.G., 1960. Toxicol. Appl. Pharmacol. 2, 44.

Shutilov, V.A., 1988. Fundamental Physics of Ultrasound. Gordon and Breach Science Publishers, Amsterdam.

Topp, M.N., 1973. Ultrasonic atomization—a photographic study of the mechanism of disintegration, Aerosol Sci. 4, 17-25.

Van Cleef, J., 1991. Powder technology. Am. Sci. 79, 304.